Research Square

Preprints are preliminary reports that have not undergone peer review.
They should not be considered conclusive, used to inform clinical practice,
or referenced by the media as validated information.

Heterologous expression of AcbHLH1 in tobacco affects trichome density and length

Jiale Tang
Hunan Horticulture Research Institute, Hunan Academy of Agricultural Sciences
Mengjie Chen
Hunan Horticulture Research Institute, Hunan Academy of Agricultural Sciences
Hai Xu
Hunan Horticulture Research Institute, Hunan Academy of Agricultural Sciences
Kejia He
Hunan Horticulture Research Institute, Hunan Academy of Agricultural Sciences
Jinshu Cai
Hunan Horticulture Research Institute, Hunan Academy of Agricultural Sciences
Rencai Wang
College of Horticulture, Hunan Agricultural University
Feixiong Luo
College of Horticulture, Hunan Agricultural University
Fanwen Bu
Hunan Horticulture Research Institute, Hunan Academy of Agricultural Sciences
Ping Yuan
yuanping@hunaas.cn

Hunan Horticulture Research Institute, Hunan Academy of Agricultural Sciences

Research Article

Keywords: bHLH, trichome, BSA-seq, kiwifruit

Posted Date: September 14th, 2026

DOI: https://doi.org/10.21203/rs.3.rs-10310012/v1

License: This work is licensed under a Creative Commons Attribution 4.0 International License.
Read Full License

Additional Declarations: No competing interests reported.

Heterologous expression of *AcbHLH1* in tobacco affects trichome density and length

Jiale Tang[1,3+], **Mengjie Chen**[1,3+], **Hai Xu** [1,3], **Kejia He**[1,3], **Jinshu Cai**[1,3], **Rencai Wang**[2,3], **Feixiong Luo**[2,3], **Fanwen Bu** [1,3*], **Ping Yuan**[1,3*],

1 Hunan Horticulture Research Institute, Hunan Academy of Agricultural Sciences, Changsha 410125, Hunan Province, China.

2 College of Horticulture, Hunan Agricultural University, Changsha, 410128, Hunan Province, China.

3 Yuelushan Laboratory, Changsha 410125, Hunan Province, China.

[+]Equal contribute

[*]Correspondence: yuanping@hunaas.cn, bufanwen@hunaas.cn

Abstract

Background As the world's largest producer and consumer of kiwifruit, China attaches significant socio-economic importance to this crop. Trichome initiation serves as a vital agronomic characteristic that provides protection against diverse biological and environmental challenges. Nonetheless, the specific functional genes governing this pathway in kiwifruit have not yet been fully elucidated. In this study, we characterized two kiwifruit lines with contrasting trichome densities: a low-density type of *A. chinensis* cv. HY-1 and a high-density type of *A. eriantha* cv. MH-1.

Results A comparative analysis of the number and density of stem trichomes between the two kiwifruit hybrid lines was then performed. BSA analysis of leaves with high trichome dengsity and low trichome density pools from the F_2 segregating population mapped the candidate genes on Chr.13. A candidate gene, *AcbHLH1*, was subsequently cloned. Phylogenetic tree analysis revealed that the protein encoded by *AcbHLH1* belongs to the atypical bHLH TF family. *AcbHLH1* was found to localize in the nucleus. The tissue-specific expression profiles of AcbHLH1 were investigated quantitative real-time PCR (qRT-PCR). Transcript accumulation was markedly higher in mature organs (leaves, petioles, stems) and floral buds, whereas expression remained relatively low in young vegetative tissues. Overexpression of *AcbHLH1* in Nicotiana tabacum caused a 37.03%–56.25% reduction in trichome density but a 70.24%–74.42% increase in trichome length on both leaves and stems.

Conclusion Taken together, our results revealed that *AcbHLH1* negatively regulates trichome density and positively regulates trichome length. This study elucidates a molecular mechanism underlying kiwifruit trichome development and provides a genetic target for breeding low-trichome kiwifruit cultivars.

Keywords:bHLH; trichome; BSA-seq; kiwifruit

Introduction

Kiwifruit (*Actinidia* spp.) is a globally significant economic crop, valued for its contribution to human nutrition and health. It is now widely cultivated commercially in major producing countries including China, New Zealand, Chile, Italy, and Iran(Richardson et al. 2018). Trichomes densely cover the stems, leaves, fruits, and other organs of kiwifruit (Sm et al. 2017). These structures provide critical protection during plant and fruit development by mitigating insect/pathogen invasion, reducing water evaporation, and minimizing mechanical damage(Amada et al. 2020; Wu et al. 2023). However, post-harvest depilation processing presents significant challenges: it frequently causes fruit skin abrasions and microtrauma that facilitate fungal colonization. This substantially increases decay rates during storage and transport, compromises fruit quality, and elevates susceptibility to post-harvest diseases(Fu et al. 2026). Addressing these challenges necessitates comprehensive elucidation of the molecular mechanisms governing trichome development.

Within *Arabidopsis* leaf epidermal cells, the tripartite MYB-bHLH-WDR (MBW) complex is assembled through the interaction of the R2R3-MYB transcription factor GLABRA1 (GL1), the bHLH factors GLABRA3 or ENHANCER OF GLABRA3 (GL3/EGL3), and the WD40-repeat protein TRANSPARENT TESTA GLABRA1 (TTG1) (Gan et al. 2011; Zhao et al. 2012). This complex binds to the promoters of downstream genes, including GL2 and TTG2, to regulate the initiation and development of trichomes (Payne et al. 2000). Among these components, GLABRA1 (GL1) was the first transcription factor identified to regulate plant trichome development (Meng et al. 2023). It acts as a key regulator that initiates trichome cell differentiation in Arabidopsis, thereby determining the formation and patterning of epidermal hairs. In *Arabidopsis*, GL1 encodes an R2R3-MYB transcription factor that functions as a key regulator in the early stage of trichome initiation. Consequently, both GL1 loss-of-function mutants and targeted knockouts of this gene lead to a glabrous (hairless) leaf phenotype (Bhandari et al. 2015). In addition, *MYB5*, *MYB23*, and *MYB82* are R2R3-MYB transcription factors that share functional similarity with GL1 and also regulate trichome elongation and branching. For example, while the *myb5* mutation leads to merely subtle variations in trichome shape (Li et al. 2009), the *myb23* knockout results in an elevated abundance of miniature and bifurcated trichomes. Additionally, the trichomeless leaf phenotype of the gl1 mutant can be functionally restored by *MYB82* (Liang et al. 2014), and similarly, *MYB23* is capable of restoring trichome formation on leaf margins and petioles in *gl1 myb23* double mutants (Kirik et al. 2005). In addition to activators, several suppressors of trichome formation have been characterized, such as TRIPTYCHON (TRY), CAPRICE (CPC), ENHANCER OF TRY AND CPC 1 (ETC1), ETC2, ETC3, TRICHOMELESS1 (TCL1), and TCL2. These R3-MYB transcription factors suppress trichome initiation

by outcompeting GL1 for binding to GL3/EGL3, which yields non-functional complexes (Wester et al. 2009; Gan et al. 2011; Feng et al. 2015). In *Arabidopsis*, ENHANCER OF TRY AND CPC 1 (ETC1) functions as a suppressor of trichome fate in both shoot epidermal cells (inhibiting trichome formation) and root epidermal cells (inhibiting the non-hair cell fate). Although loss of ETC1 alone causes minimal trichome defects, it enhances the phenotypes of *cpc* and *try* mutants, supporting its cooperative role in trichome repression (Kirik et al. 2004). Separately, TCL1 also negatively regulates trichome initiation, with its overexpression shown to directly inhibit GL1 expression (Wang et al. 2007).

Actinidia species exhibit high genetic diversity, with trichome types on stems, leaves, and fruit surfaces varying widely (White 1986a). These trichomes include glabrous, pubescent, tomentose, bristly, and scabrous forms. Distinct differences in trichome structure are evident across various cultivars. For instance, small, two-celled uniseriate hairs cover the surface of *Actinidia rufa*. In contrast, *Actinidia eriantha* and *Actinidia deliciosa* display a combination of large multiseriate and small, two-celled uniseriate trichomes (White 1986b). Zheng et al analyzed 56 kiwifruit varieties and identified 327 single nucleotide polymorphisms (SNPs) as well as 260 haplotypes associated with fruit hairiness. These genetic variants were found in genes implicated in protein function, membrane composition, and metabolic pathways related to stress resistance (Zheng et al. 2022). A study revealed a correlation between ploidy level and trichome characteristics in kiwifruit, with polyploid cultivars exhibiting significantly greater trichome length and density. Transcriptomic analysis further identified 235 differentially expressed genes (DEGs), which were enriched in hormone signaling pathways and flavonoid biosynthesis (Qi et al. 2026). Short and distorted trichome phenotype observed in *Actinidia latifolia* is potentially attributable to the combined effects of transcriptional suppression and alternative splicing of the *AlNAP1* gene (Miao et al. 2023). Despite preliminary insights into the trichome morphology and molecular mechanisms of kiwifruit trichome morphogenesis, the regulatory networks governing trichome initiation and differentiation remain incompletely characterized. Further systematic investigation is required to elucidate the molecular regulatory systems controlling kiwifruit trichome development.

The bHLH transcription factor serves as a central regulator in the trichome development network (Méndez-Vigo et al. 2024). Although bHLH proteins (e.g., GL3/EGL3) cannot independently initiate trichome morphogenesis, they function as core scaffolding components. Together with the MYB factor GL1 and WD40 protein TTG1, they form an MBW complex that activates downstream genes to precisely control trichome initiation and differentiation (Morohashi and Grotewold 2009). Conversely, inhibitory R3-MYB factors competitively bind bHLH proteins

(GL3/EGL3), displacing the activator GL1 (R2R3-MYB). This prevents assembly of functional MBW complexes, thereby suppressing trichome formation (Ahmad Khan et al. 2024). This molecular insight establish bHLH TFs as the main regulatory factors in controlling trichome development in plants. However, the role of bHLH TFs in kiwifruit trichomes remains unexplored.

Here, we report the identification of *AcbHLH1*, a novel bHLH transcription factor, as a putative regulator of trichome formation. This gene was identified through bulked segregant analysis (BSA) resequencing of an extreme-phenotype population. The population was a BC_1 generation derived from crossing the high-trichome-density *A. eriantha* cv. MH-1 (maternal parent) with the low-trichome-density *A. chinensis* cv. HY-1 (paternal parent). Subcellular localization analysis revealed that *AcbHLH1* resides in the nucleus. When heterologously expressed in tobacco, this gene led to a marked decrease in trichome density on both leaves and stems. This study deciphers the molecular mechanism underlying kiwifruit trichome development, identifying potential genetic targets for breeding low-trichome varieties.

Results

Phenotypic diferences of trichomes in kiwifruit accessions

The trichome distribution patterns on young stems of *A. chinensis* cv. HY-1 and *A. eriantha* cv. MH-1 were compared (Figure 1A). The young stems of HY-1 exhibited sparse coverage of low density trichomes, whereas those of MH-1 showed dense coverage of high density, intertwining trichomes, which were significantly higher than those of HY-1 (Figure 1B). Due to the distinct morphological characteristics of the HY-1 and MH-1 trichomes, we constructed an F1 hybrid progeny population using the MH-1 plants as the maternal parent and HY-1 plants as the paternal parent. Based on this, we further constructed a BC_1 hybrid population using the F_1 hybrid progeny individual MZ-69 as the maternal parent and HY-1 plant as the paternal parent. The results showed that the length and density of trichome on MH-1 and MZ-69 plants were significantly greater than those on HY-1 plants (Figure 1 C, D). Moreover, the sprouting days were numbered from 10 to 60 according to the growth order, meaning that Day 10 marked the initial stage of the plant's stem development after sprouting. The results showed that the young stems of MH-1 plants were covered with high density trichomes during the 60-day germination period, while the HY-1 plants had low density trichomes during the same period, and the density of trichome began to decrease after 40 days of germination (Figure 1 E). Therefore, this study chose to measure the density of trichome during the 40-day germination period of young stems to represent their characteristics. We measured trichome density in HY-1 and MH-1

parental lines (n=9 plants per line), 89 F_1 hybrids, and 232 BC_1 progeny to determine the genetic basis of these traits using segregation analysis. The average trichome length of trichome in HY-1 was 239.2 number/mm^2, in MH-1 was 889.6 number/mm^2, and in F1 was 594.5 number/mm^2. (Figure 1F). Furthermore, the segregation of trichome trait in the BC_1 population were also observed in young stems. The average trichome length of trichome in 232 BC_1 individuals was 384.30 number/mm^2, and exhibited a continuous frequency distribution with a range of 130.03-954.68 number/mm^2 (Fig. 1G).

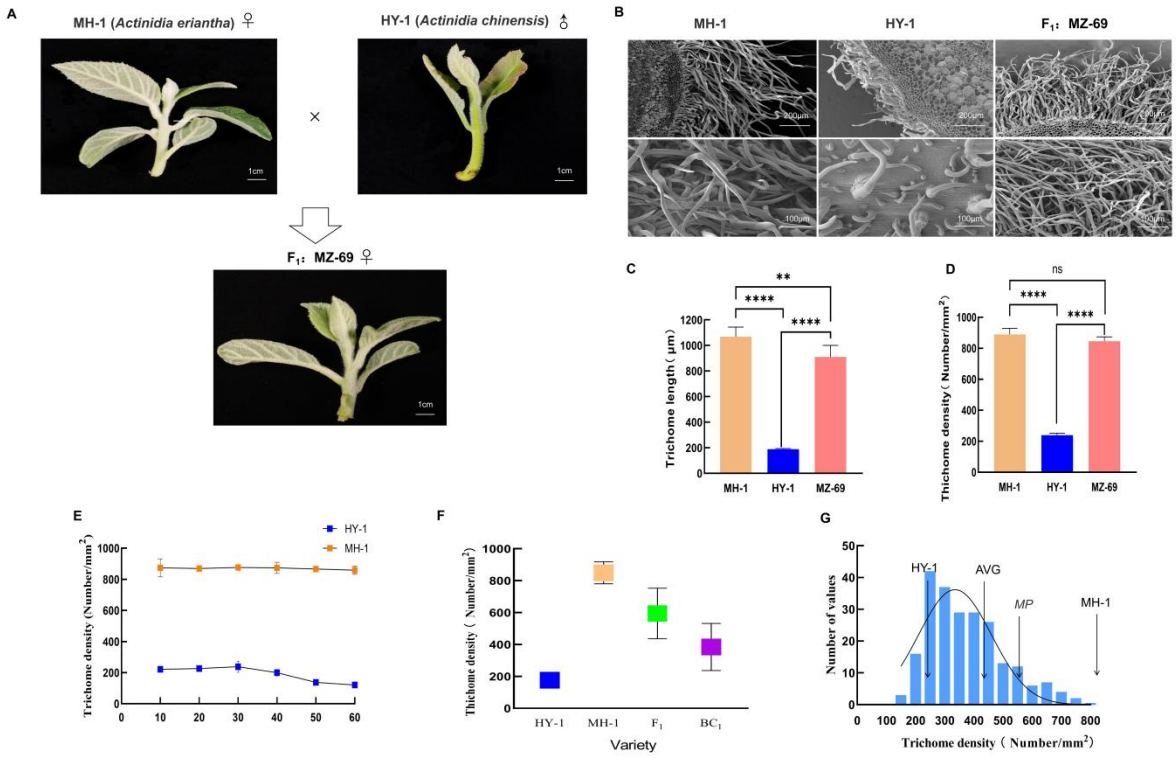


Figure 1 Trichome trait phenotypes of the selected parent lines and their progenies.
A: Trichome trait of MH-1, HY-1 and MZ-69 on their stem, the scale on the right represents the length of 1 cm. B: Microscopy observation of trichomes on the stems of MH-1, HY-1 and MZ-69 plants. C: The trichome length on stem in MH-1, HY-1 and MZ-69 plants. Error bars represent the standard error of the mean (n = 9). D: The trichome density on stem in MH-1, HY-1 and MZ-69 plants. Error bars represent the standard error of the mean (n = 5). Different letters on top of bars indicate significant differences between treatments (**: p<0.005; ****: p<0.0001; ns: not significan). E: Trichome dengsity on stem of MH-1 and HY-1 plants after germination of 10-60 days. Values are means ± SD (n = 3). F: Statistics of trichome density on the 40 day stems of MH-1, HY-1, F_1 and BC_1 plants. Values are means ± SD (n = 9). G: Frequency distribution of trichome density among 232 BC_1 individuals. Population Average value: AVG; Mid-parent value: MP.

Selection of Candidate Region

In order to further explore the candidate genes that regulate the formation of trichomes, we used the BSA-Seq strategy to identify candidate regions and find genes

related to the formation of trichomes. After screening to remove low-quality reads, a total 41.98 Gb clean data were obtained from the two bulks for further analysis 21.24Gb for the high density (HD) bulk and 20.73 Gb for the low density (ST) bulk. The average Q30 ratio of four samples was 94.05% and the average GC content of four samples was 36.44%. The genome resequencing depth with an average > 36× and genome coverage > 81% (Table S1). After filtering of this raw data, a total of 3,340,108 SNPs was obtained and a Δ (SNP-index) was indicated by calculating SNP-index. seven candidate intervals exceeded the threshold value and located on chromosome group13 of *Actinidia_chinensis* (Figure 2, Table S2). Together, the candidate regions were contain a total of 5.7 Mb with approximately 146 annotated genes (Table S3). We found 999 SNPs with non-synonymous coding between the parents, and 544 SNPs with non-synonymous coding across these genes between the two bulks（Table S4）. These SNPs and indels are likely to be directly associated with trichomes. In summary, this results show that the candidate genes for trichome density were located on chromosome group 13 of *Actinidia_chinensis.*

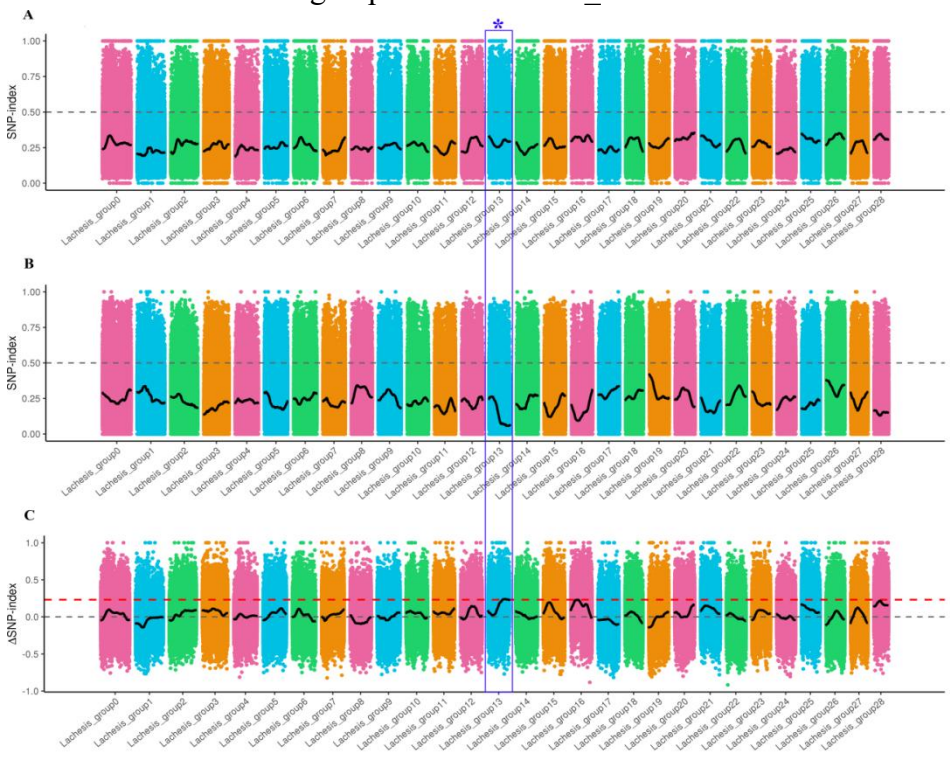


Figure 2 The layout of SNP index and ΔSNP Index

A: The distribution of SNP index of the short trichome length bulk from the BC_1 population. B: The distribution of SNP index of the long trichome length bulk from the BC_1 population. C: The layout of Δ(SNP Index) value. The x-axis and y-axis represent the 29 kiwifruit chromosomes in two bulk-genomes and the SNP index, respectively. The solided curve line indicates the fitted SNP index or ΔSNP index. The red dotted horizontal line indicates the association threshold of 99% confidence interval.

Transcriptome Profiling of Trichome Development in Kiwifruit

To investigate the potential mechanism underlying the formation of multiple trichomes in kiwifruit, we performed transcriptome profiling via RNA-seq using 40-day-old young stems of *A. chinensis* (HY-1) and *A. eriantha* (MH-1). Sequencing yielded 41.06 to 47.03 million clean reads per sample, which were subsequently aligned to the complete genome sequence of kiwifruit Hong Yang v3. Principal component analysis (PCA) revealed significant divergence between the two comparative groups (Figure 3A). Using a false discovery rate (FDR) < 0.01 and |log2(fold change)| > 1 as thresholds for identifying differentially expressed genes (DEGs), a total of 9,781 DEGs were detected between HY-1 and MH-1. Among these, 5,145 genes were up-regulated and 4,636 were down-regulated (Figure 3B、C).

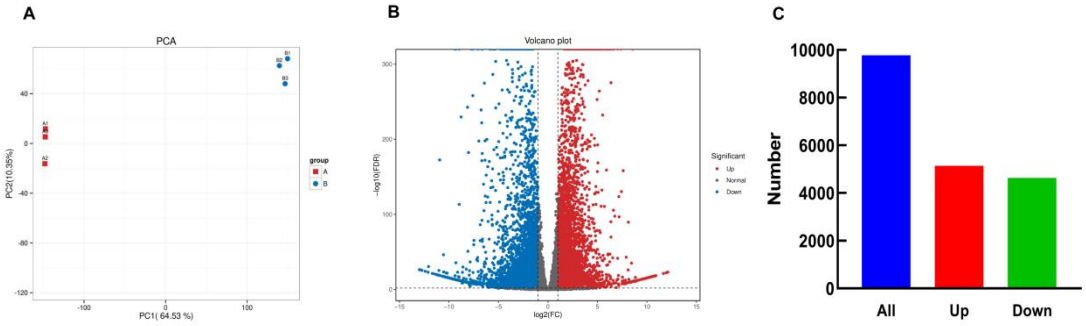


Figure 3 Principal components analysis, volcano diagrams and bar chart diagrams of differentially expressed genes (DEGs)

A: Principal component analysis of HY-1 and MH-1. B: Differentially expressed genes in stem between HY-1 and MH-1. C: The nμmber of differentially expressed genes HY-1 and MH-1.

Identify the Key Genes Related to Trichome Development in kiwifruit

In order to further explore the key genes affecting the plant trichome development of kiwifruit, the results by BSA-seq and RNA-seq were combined to analyze. We Compared the 146 candidate genes obtained by BSA-seq with the 9781 DEGs obtained by RNA-Seq using the Venn diagram to obtain common genes among them (Table S5). As shown in figure 4, a total of 35 common genes were annotated within the candidate intervals (Table S6). Furthermore, KEGG pathway enrichment analysis of genes indicated that these genes were mainly enriched in DNA replication, homologous recombination, mismatch repair, nucleotide excision repair, basal transcription factors, amino sugar and nucleotide sugar metabolism and pyrimidine metabolism (Figure 5).

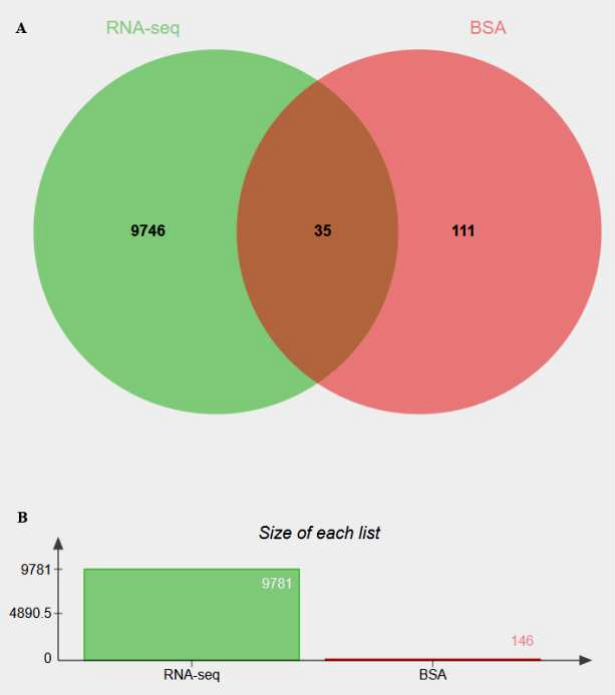


Figure 4 Venn diagram of RNA-seq data combined with BSA data

A: Venn diagram depicting the nµmber of all annotated genes in RNA-seq data and BSA data. B: Total nµmber of annotated genes identified for RNA-seq data and BSA-seq data. green color indicates DEGs in RNA-seq data and red color indicates annotated genes in BSA-seq data.

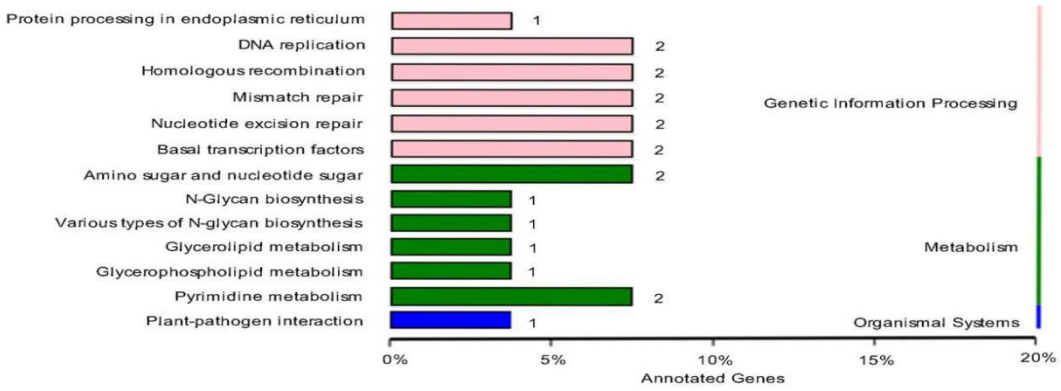


Figure 5 The Sµmmary of KEGG classification of the annotated genes

Pink, green, blue indicates genetic information processing, metabolism, organismal systems annotated genes, respectively.

Comparative sequence analysis of the candidate *AcbHLH1* and *AcbHLH1* genes

Then, we amplified and comparatively analyzed the genomic and coding sequences of the *AcbHLH1* and *AebHLH1* genes from the *A. chinensis* cv. HY-1 and *A. eriantha* cv. MH-1 plants, respectively. The amino acid sequences of *AcbHLH1* and *AebHLH1* were 276 residues in length. *AcbHLH1* shared 98.91% amino acid sequence similarity

with *AebHLH1*. Sequence analysis revealed that three SNPs were present between the two alleles of the bHLH1 gene from the low density trichomes parent HY-1 and the high density trichomes parent MH-1, which resulted in three amino acid changes, at positions 23 (tyrosine to phenylalanine) , 36 (leucine to phenylalanine) and 135 (arginine to lysine) (Figure 6A). The protein sequences of *AcbHLH1* and *AebHLH1* were used to identify their homologous sequences. *AcbHLH1* and *AebHLH1* were located in the same clade as other trichome-related bHLH genes in kiwifruit (Figure 6B). These results revealed that both *AcbHLH1* and *AebHLH1* encodes a putative bHLH transcription factor in kiwifruit .

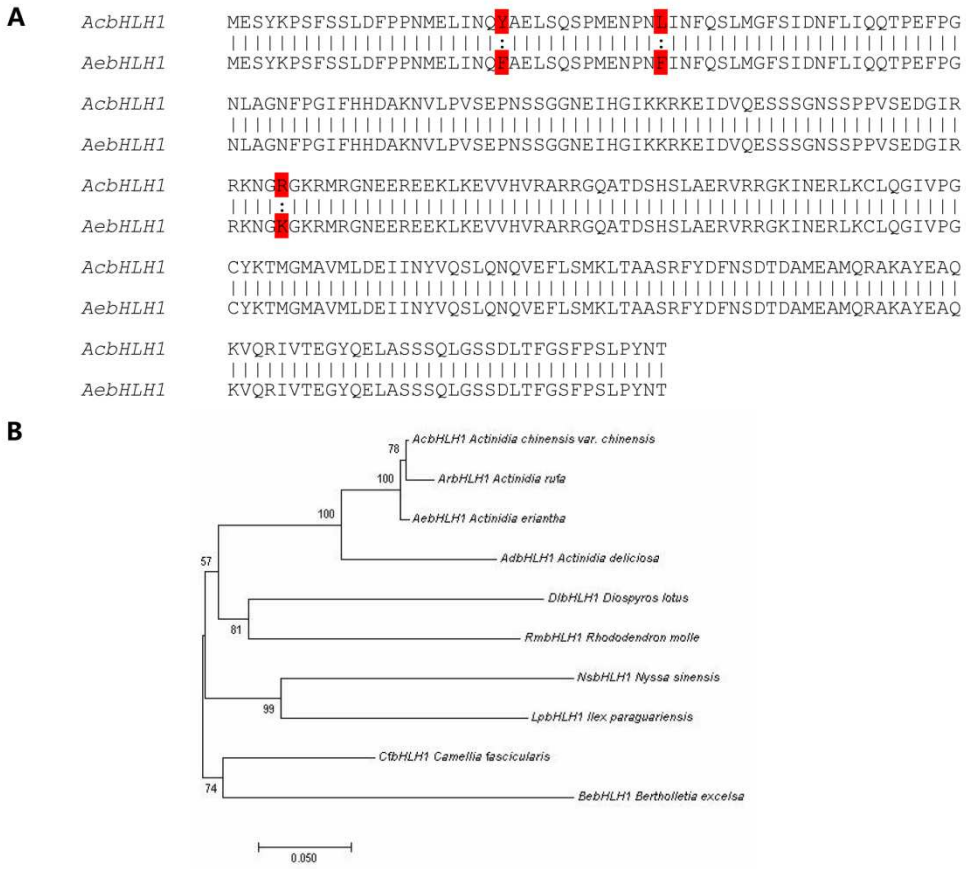


Figure 6 Gene structure and phylogenetic analysis of *AcbHLH1* and *AebHLH1*

A. Gene structure of bHLH1 and polymorphisms between *AcbHLH1* from *A.chinensis* and MH-1 plant from *A. eriantha*. B. Phylogenetic analysis of *AcbHLH1* and *AebHLH1* and their homologs.

AcbHLH1 highly expressed in low density trichomes and subcellular located in nucleus

In order to explore the expression pattern of *AcbHLH1*, the transcription expression levels of the *AcbHLH1* in low density trichomes (HY-1) and high density trichomes MH-1 were detected. The transcript levels of bHLH1 were significantly higher in the

low-density plant HY-1 than in the high-density plant MH-1(Figure 7A). However, from 20 days after germination, the transcription expression level of the *AcbHLH1* gene in the stems of HY-1 plants significantly increased (Figure 7B). Moreover, the different tissues(young leaves, young leafstalks, young stems, and mature leaves, mature leafstalks, mature stems, and mature buds) were used for quantitative reverse transcription qRT-PCR analysis. Compared to its expression in young leaves, leafstalks, young stems, and early buds, the *AcbHLH1* gene exhibits higher expression levels in mature leaves, mature leafstalks, mature stems, and mature buds (Figure 7C). These results suggest that the *AcbHLH1* gene regulates the formation of trichomes in various organs of kiwifruit. To determine the subcellular localization of *AcbHLH1*, we transiently expressed a GFP-tagged fusion protein in *Nicotiana benthamiana* leaves via Agrobacterium-mediated transformation. Confocallaser scanning microscopy confirmed the nuclear localization of *AcbHLH1*-GFP, consistent with its predicted role as a transcription factor (Figure 8).

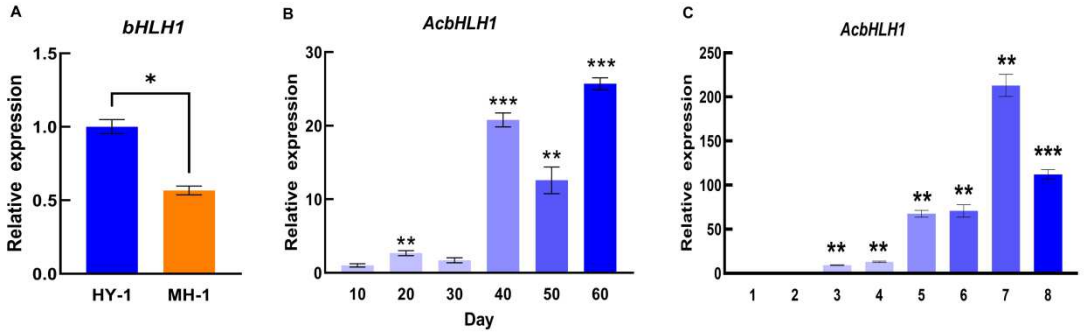


Figure 7 Relative transcript expression levels of bHLH1 gene

A: Expression levels of bHLH1 gene between the stems with low density trichomes from HY-1 plant and stems with high density trichomes from MH-1 plant, after germination of 40 days. B: Expression levels of *AcbHLH1* between the stems short trichomes from HY-1 plant, after germination of 10-60 days. Values are means ± SD (n =3). C: Expression levels of *AcbHLH1* among different tissues from HY-1 plant . 1–4 represent the leaves, leafstalk, stems, and flower buds, respectively, from HY-1 plant at the seedling stage; 5–8 represent the stems, old leave from HY-1 at the flowering stage. Different letters on top of bars indicate significant differences between treatments (*: p<0.05; **: p<0.005; ***: p<0.0005).

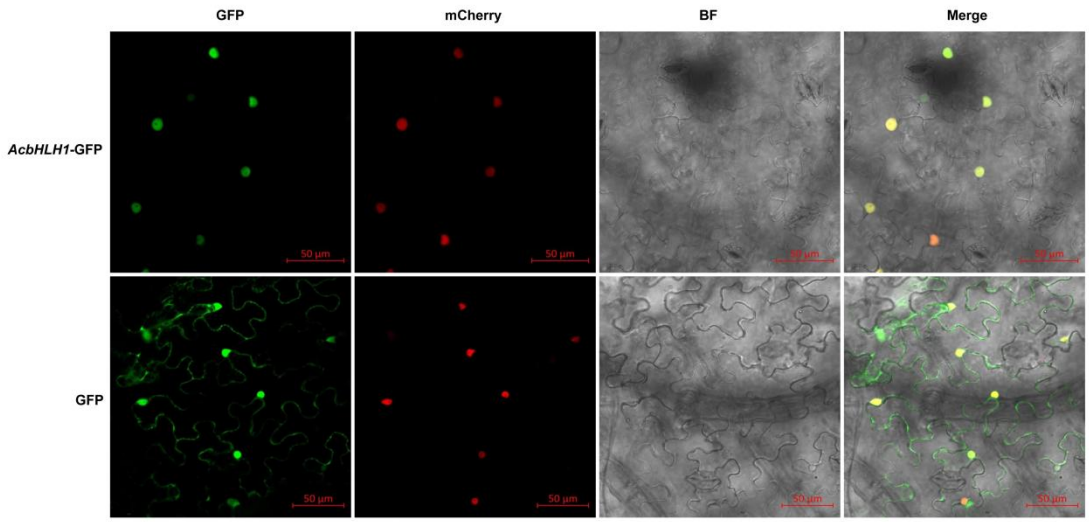


Figure 8 Nuclear localization of *AcbHLH1* gene in N.*benthamiana* leaves

Transient expression of *AcbHLH1*-GFP tagged fusion proteins in Nicotiana *benthamiana* (72 h post-infiltration). GFP was used as nuclear marker; Images show GFP, mCherry, bright-field, and merged channels, Scale bar =50μm.

Overexpression *AcbHLH1* resulted in decreased trichome density and increased trichome length in tobacco

To investigate the functional role of *AcbHLH1* in trichomes development, we constructed overexpression lines, designated as *AcbHLH1*-OE (Figure 9A). Therefore, we extracted genomic DNA from T_2 generation tobacco plants and performed PCR amplification identification. The results showed that the T_2 generation plants could successfully amplify the target fragment (831bp), indicating that the *AcbHLH1* gene had been successfully transferred into tobacco (Figure 9B). Moreover, validated the gene expression levels in T_2 generation plants using qRT-PCR. Among the over expression lines, OE-2 exhibited the highest transgene expression level (13.76-fold increase compared to wild-type), followed by OE-3 (13.45-fold) (Figure 9C).

Stereoscopic images were taken of the leaves at the same position on plants from both the control group and the overexpression line, as well as the morphology of trichomes at the same location(Figure 10A, E). Scanning electron microscopy results revealed that in the stem region of the *AcbHLH1* overexpressing line, some trichomes exhibited longer lengths and thicker bases compared to wild-type trichomes, with a length of approximately 250μm(Figure 10B, C, F, G). Through statistical analysis of the length and density of stem trichomes, the average density of trichomes in the *AcbHLH1* overexpressing line was 56.00 number/mm^2, while the density in the wild-type line was 128.00 hairs/mm^2 (Figure 10D). The average length of trichomes

in the *AcbHLH1* overexpressing lines was 262.84μm, whereas the length in the wild-type lines was 150.69μm (Figure 10H). In summary, overexpression of *AcbHLH1* resulted in a 56.25% reduce in trichome density on tobacco stems while increasing trichome length by 74.42%.

Moreover, Stereoscopic images were taken of the leaves at the same position on plants from both the control group and the overexpression line, as well as the morphology of trichomes at the same location (Figure 11A, E). Observations of trichomes on tobacco leaf surfaces revealed significant differences in both density and length of the leaf trichomes in the *AcbHLH1*-OE line compared to the wild-type (WT) of *Nicotiana benthamiana* (Figure 11B, C, F, G). The results show the average density of trichomes in the *AcbHLH1* overexpressing line was 22.67 number/mm^2, while the density in the wild-type line was 36.00 number/mm^2 (Figure 11D). The average length of trichomes in the *AcbHLH1* overexpressing lines was 315.31μm, whereas the length in the wild-type lines was 185.22μm (Figure 11H). In summary, overexpression of *AcbHLH1* resulted in a 37.03% reduce in trichome density on tobacco leaves while increasing trichome length by 70.24%.

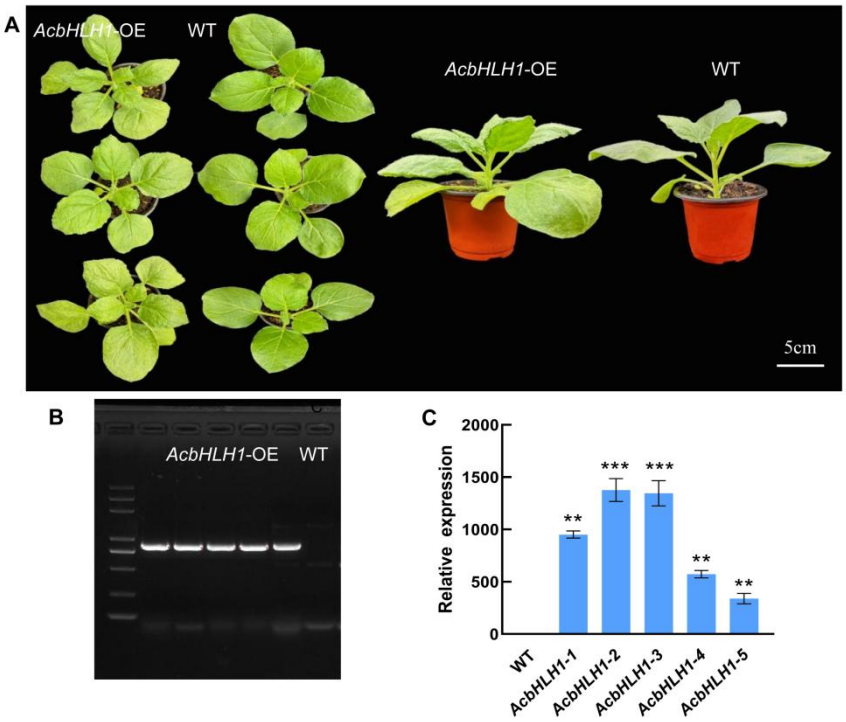


Figure 9 Molecular identification of *AcbHLH1* overexpression lines in Nicotiana *benthamiana*.

WT: Nicotiana *benthamiana* wild type. *AcbHLH1*-1~5: *AcbHLH1* overexpression lines. A: Tobacco leaf morphology. B: DNA insertion analysis. C: Transcriptional level analysis (**: p<0.005; ***: p<0.0005）.

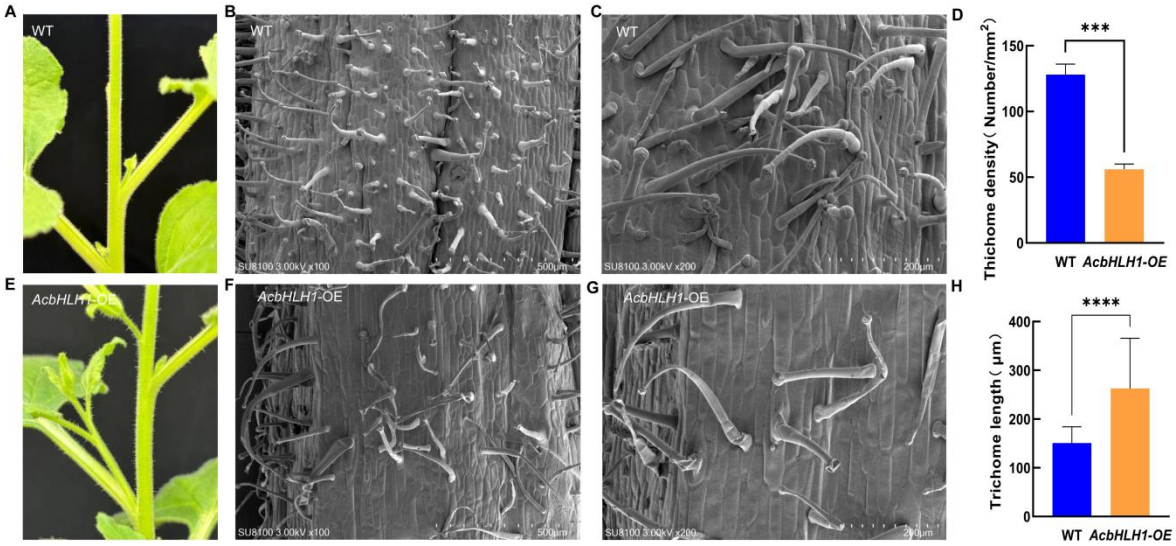


Figure 10 Identification analysis of trichome density and length on the stem in *AcbHLH1*-OE tobacco

A, E: The morphology of the stem between the fifth and sixth at the top of tobacco. B, C: SEM images of the stem on WT Tobacco plants. F, G: SEM images of the stem on *AcbHLH1*-OE transgenic plants. Scale bars represent 500 μm and 200 μm, respectively. D: The trichome density on the stem in Tobacco plants. H: The trichome length on stem in tobacco plants. Error bars represent the standard error of the mean (n = 9). Different letters on top of bars indicate significant differences between treatments (***: p<0.0005; ****: p<0.0001).

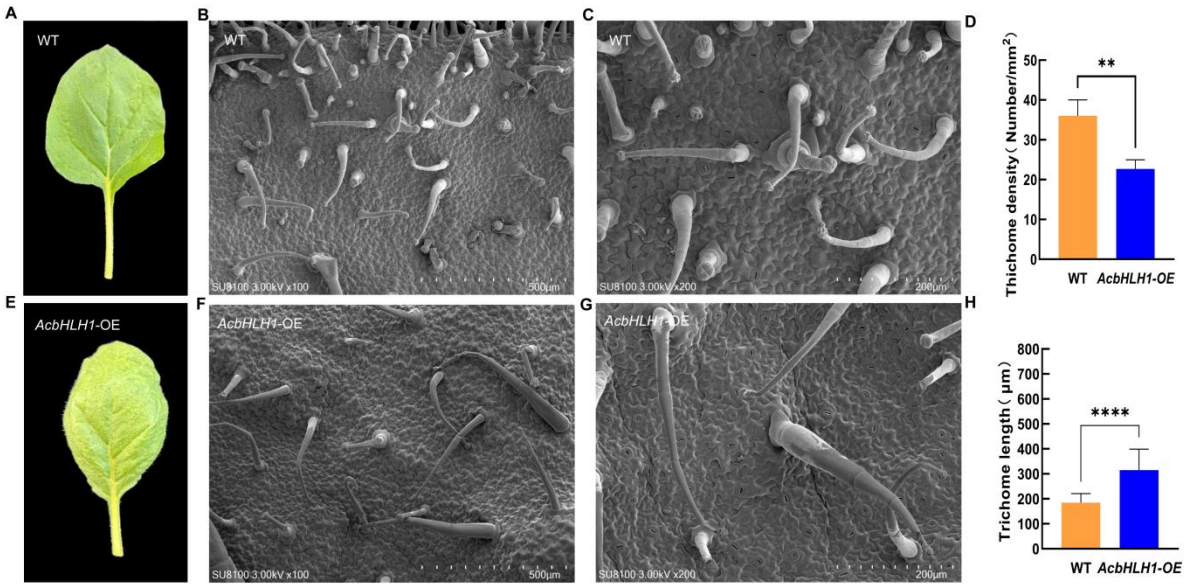


Figure 11 Identification analysis of trichome density and length on the upper epidermis of leaves in *AcbHLH1*-OE tobacco

A, E: The morphology of the fifth leaf at the top of tobacco. B, C: SEM images of the upper epidermis of leaf on WT tobacco plants. F, G: SEM images of the upper epidermis of leaf on *AcbHLH1*-OE transgenic plants. D: The trichome density on the upper epidermis of leaf in Tobacco plants, Scale bars represent 500 μm and 200 μm, respectively. H: The trichome length on the dowm epidermis of leaf in Tobacco plants. Error bars represent the standard error of the mean

(n = 9). Different letters on top of bars indicate significant differences between treatments (**: $p<0.005$; ****：$p<0.0001$).

Discussion

Trichome density on plant surfaces is closely associated with resistance to diseases and insect pests, and also significantly affects the appearance quality of kiwifruit (Alahakoon et al. 2016). Kiwifruit with smooth, clean, and hairless skin are generally more preferred by consumers (Harker et al. 2007). Nevertheless, a comprehensive understanding of the molecular pathways governing kiwifruit trichome initiation and growth is still lacking. This study aims to identify the key regulators of trichome formation in kiwifruit. Previous transcriptomic analyses of trichome and trichome-free leaves have identified TFs associated with trichome growth (Heng et al. 2025). For instance, transgenic suppression of glandular trichome abundance in tobacco via *NtMYB306c* hyper-expression was documented by Zheng et al (Zheng et al. 2025). Concurrently, R2R3 MYB-mediated auxin pathways govern trichome development, with increased trichome numbers providing tomato crops with defense against spider mites (Yuan et al. 2021). In this study, we cloned and characterized the *AcbHLH1* gene from kiwifruit, which was first identified through BSA analysis of leaf tissues exhibiting either high or low trichome density. Quantitative RT-PCR validation further showed that *AcbHLH1* transcripts are more abundant in low-density trichome tissues than in high-density trichome tissues. Sequence homology and phylogenetic analyses indicated that *AcbHLH1* encodes a typical bHLH transcription factor harboring canonical DNA-binding domains. The *AcbHLH1* protein was found to reside solely within the nucleus, as demonstrated by subcellular localization analysis. Moreover, functional assays in tobacco demonstrated that *AcbHLH1* acts as a negative regulator of trichome density.

The bHLH transcription factor serves as a core component of the MBW complex, which plays a critical role in promoting epidermal hair development (Peng et al. 2025). Studies in *Arabidopsis* have shown that bHLH transcription factors, including GL3 and EGL3, interact with MYB transcription factors (e.g., GL1) and the WD40 repeat protein TTG1 to form a heterotrimeric MYB-bHLH-WD40 complex. This complex activates the expression of the downstream gene GL2, thereby initiating the differentiation of epidermal hair cells (Payne et al. 2000; Morohashi et al. 2007). In rapeseed (*Brassica napus*), for instance, the overexpression of the *AtGL3* gene suppresses *BnTTG1* expression. This suppression promotes trichome growth and elongation(Alahakoon et al. 2016). The current investigation reveals that bHLH-type TFs play a vital role that goes beyond merely governing trichome morphogenesis in *Arabidopsis* and *Brassica napus*, but they are also involved in this process in kiwifruit (Payne et al. 2000; Heydarian et al. 2024). These observations align closely with what

has been documented in recent studies regarding the alleles of *BnGL3* and *BrGL3* and *BvGL3*-a bHLH family gene from soybean (*Glycine max*)-in which ectopic expression of these genes induced trichome formation in glabrous *Brassica napus,* with the resulting trichome number being commensurate with the trichome density of the original donor accessions (Heydarian et al. 2024). Similarly, in *Artemisia annua*, the *AaGL3* gene, which is homologous to *AtGL3* (GLABRA3), positively regulates trichome density (Ahmad Khan et al. 2024). Numerous studies have shown that loss of GL3 or EGL3 function leads to a marked reduction in the number of trichomes in plants, indicating their irreplaceable role in development. For example, The bHLH transcription factor gene EGL3 (also known as MAU1) affects the surface coat distribution pattern on *Arabidopsis* fruits through synergistic interactions with the MYB genes TRICHOELESS1, GLABRA1, and TRY (Méndez-Vigo et al. 2024). In *Arabidopsis thaliana*, GL3 and EGL3 are well-characterized bHLH genes. Single mutants of GL3 or EGL3 exhibit reduced epidermal hair number and branching, whereas the double mutant displays a completely glabrous (hairless) phenotype (Méndez-Vigo et al. 2024). Overexpression of *MYC1* (a bHLH gene) doubles the number of epidermal hairs, while mutation of *MYC1* reduces it (Fambrini and Pugliesi 2019). In addition, knockout of *NtMYC2*, a bHLH gene in tobacco, results in reduced density of both long and short glandular trichomes on leaves and complete loss of non-secretory epidermal hairs (Zhao et al. 2012). These findings indicate that bHLH genes play an essential role in regulating trichome development in plants.

The precise regulation of the density and distribution of plant trichomes is critical for plant adaptation to the environment (Yu et al. 2025). This process is governed by a multi-level transcriptional regulatory network, in which negative feedback regulation mediated by bHLH transcription factors constitutes a core mechanism for maintaining trichome homeostasis and preventing excessive formation. bHLH transcription factors serve as key targets of R3-MYB repressors (Wester et al. 2009). R3-MYB transcription factors competitively bind to bHLH proteins (e.g., GL3/EGL3), thereby inhibiting the formation of MBW complexes and providing negative feedback that restricts trichome overgrowth (Feng et al. 2015). In addition, some bHLH transcription factors can independently negatively regulate trichome density. They achieve this by forming multiple negative feedback loops through direct repression of target genes, modulation of hormone synthesis, or interaction with other factors, thereby fine-tuning epidermal hair development(Payne et al. 2000). This study demonstrates that overexpression of kiwifruit *AcbHLH1* in tobacco significantly reduces upper leaf and stem trichome density, directly showing that bHLH family members can act as both positive and independent negative regulators within MBW complexes, thereby fine-tuning trichome density via bidirectional regulation. These

results align with previous observations regarding *NtPRE4.1*, a separate bHLH family gene documented to exert a negative regulatory effect on tobacco trichome density. Functional validation showed that overexpression of *NtPRE4.1* reduced tobacco glandular trichome density by 40–48%. When *NtPRE4.1* was knocked down by virus-induced gene silencing (VIGS), glandular trichome density significantly increased by 44–69% compared with the control (Heydarian et al. 2024). At the molecular level, *NtPRE4.1* interacts with *NtMYB33*0 (an R2R3-MYB protein specifically expressed in epidermal hairs) and inhibits its transcriptional activation activity. In addition, *NtPRE4.1* downregulates gibberellin (GA) biosynthesis-related genes, thereby blocking trichome initiation through both protein-protein interaction and hormone signaling pathways (Yang et al. 2025). Similarly, tomato *SlbHLH95* is a typical negative regulator of epidermal hairs, and its expression pattern is highly correlated with its function (Chen et al. 2020). *SlbHLH95* expression is extremely low in stems with high-density epidermal hairs, whereas overexpression of *SlbHLH95* leads to a marked decrease in stem epidermal hair density. Mechanistic studies have confirmed that *SlbHLH95* can directly bind to the promoters of two key gibberellin synthesis genes, *SlGA20ox2* and *SlKS5*, and inhibit their transcription, thereby reducing the active GA content in plants. Furthermore, exogenous GA treatment restores the reduced phenotype of the *SlbHLH95* over expression line, indicating that *SlbHLH95* negatively regulates trichome density by suppressing GA biosynthesis.

Therefore, bHLH transcription factors form a multi-level negative feedback regulatory network by participating in the MBW positive regulatory complex, mediating competitive inhibition by R3-MYB proteins, and independently regulating hormone synthesis and target genes. This network represents the core mechanism for the precise control of plant epidermal hair density. Future research should further elucidate the upstream regulation of bHLH negative regulators, their interaction networks with other transcription factors (e.g., HD-ZIP, C2H2), and strategies for precisely modulating kiwifruit epidermal hair density via gene editing, thereby providing a theoretical basis for breeding varieties with reduced trichome density.

Conclusions

This study generated a BC_1 population by backcrossing high-density trichome plants (MZ-69, selected from an F_1 population) as the maternal parent with low-density trichome kiwifruit (*Actinidia chinensis* cv. HY-1) as the paternal parent. Phenotypic identification of trichome length and density was performed on the BC_1 population. Extreme-phenotype bulks (high vs. low trichome density) were constructed for bulked segregant analysis (BSA) coupled with whole-genome resequencing. SNP association analysis using the SNP-index method identified a major quantitative trait locus (QTL) for trichome density on chromosome 13. Differential gene expression analysis of

RNA-seq data within this QTL interval identified *AcbHLH1* as the primary candidate gene, based on significant sequence variations and expression differences. Subsequent analysis of its deduced amino acid sequence, promoter region, and transcriptional expression profile facilitated the construction of an *AcbHLH1* overexpression vector. Heterologous overexpression of *AcbHLH1* in tobacco yielded transgenic lines exhibiting significantly reduced trichome density and significantly increased trichome length on stems and leaves compared to controls. These results demonstrate that *AcbHLH1* negatively regulates trichome density and positively regulates trichome length. This study elucidates a molecular mechanism underlying kiwifruit trichome development and provides a genetic target for breeding low-trichome kiwifruit cultivars.

Materials and Methods

Plant Materials and Phenotyping for Trichomes

Samples of *Actinidia chinensis* cv. HY-1 and Ac*tinidia eriantha*a cv. MH-1 were acquired from Hunan Province, China, during [2020/12]. The botanical materials were officially authenticated by assistant researcher Jiale Tang (Hunan Horticulture Research Institute, Hunan Academy of Agricultural Sciences). To facilitate future reference, voucher specimens (Ac-2020-01 and Ae-2020-03) were deposited in the Herbarium of the Institute of Botany at the Hunan Horticulture Research Institute. Two kiwifruit species, *Actinidia chinensis* cv. HY-1 which had low trichome density young stems, and *Actinidia eriantha* cv. MH-1 which had young stems which had high trichome density, were used as parental lines to generate F_1 population. In September 2017, 89 F_1 hybrid seedlings were grown in the experimental field. F_1 population MZ-69 individual and *Actinidia chinensis* cv. HY-1 were crossed, and generated BC_1 population for BSA. A total of 232 BC_1 individuals were grown in 2023. To confirm the phenotypes, 20 natural varieties were plant in 2020, each variety planted three individuals as biological repetition. All plant materials were cultivated at the experimental farm of the Hunan Provincial Horticulture Research Institute and managed according to standardized practices for irrigation, fertilization, and pest and disease control.

Evaluation of trichome phenotypes

The trichome density of young stems in two parental lines on every sprouting days was evaluated during 2023, after taking the photographs of young stems under a scanning electronic microscope (SEM), the length and density of trichomes were calculated using a $1mm^2$ grid and ImageJ-Win64 software. The statistically

significance of differences between mean values of each parental lines was obtained by GraphPad Prism version (v9.5). The BC_1 population was grown in plastic pots (10 cm in diameter × 12 cm in height) filled with a medium containing nutrient soil (Xianghuinongke, China) and vermiculite (Baituji, China) mixed in a 2:1 (v/v) ratio under standard growth conditions. The BC_1 population was phenotyped over two consecutive growing seasons (2024-2025). Trichome length on juvenile stems (40-day post-sprouting) was quantified per plant using stereo microscopy, with data collected for BSA sequencing of trichome-related traits. The trichome length frequency distribution histogram of the 232 BC_1 individuals was drawn by GraphPad Prism version (v9.5) using the method of nonlinear regression. The trichome density of natural population were the means of three biological repetition for each variety. All results were the means of six independent replicates per treatment.

DNA isolation and bulked segregant analysis sequencing

Young healthy leaves were collected from *Actinidia chinensis* cv. HY-1, *Actinidia eriantha* cv. MH-1 and BC_1 population. Total genomic DNA was extracted using the CTAB method. The DNA integrity and purity were assessed through agarose gel electrophoresis. Additionally, DNA purity was determined by NanoDrop spectrophotometry based on the OD260/OD280 absorbance ratio. For BSA-seq, 25 short trichome length plants and 25 long trichome length plants were selected from BC_1 population and an equal amount of DNA from each plant in each response group were pooled as the high density trichome pool (HD-pool) and low density trichome pool (LD-pool), and individual *Actinidia chinensis* cv. HY-1 and *Actinidia eriantha* cv. MH-1 plants were used to establish parental pools. The concentration of DNA of parents, HD-pool and LD-pool was adjusted to 50 ng μL^{-1}. Biomarker Technologies (Beijing, China; www.biomarker.com.cn) performed paired-end resequencing (2×150 bp, 30× coverage) of the four DNA pools using the Illumina NovaSeq 6000 platform. The reference genome is the complete genome sequence of kiwifruit Hong Yang v3 (https://kiwifruitgenome.org). The raw sequencing sequence obtained from high-throughput sequencing is subjected to sequencing data quality control, and the Clean Reads obtained from sequencing are repositioned onto the reference genome. Then, the GATK software toolkit is used for SNP (Single Nucleic Polymorphism) detection and annotation (McKenna et al. 2010). Perform SNP association analysis based on SNP index algorithm to explore and discover genetic loci and use Δ(SNP index) statistics (Takagi et al. 2013; Fekih et al. 2013). The calculation formula for the SNP index method is as follows.

$$SNP\ index(aa)=Maa/(Maa+Paa) \quad (1)$$

$$SNP\ index(ab)=Mab/(Mab+Pab) \quad (2)$$

$$\Delta SNP\ index = SNP\ index(aa)- SNP\ index(ab) \quad (3)$$

In the formula, Maa represents the depth of the aa pool (recessive mixed pool) derived from the recessive parents; Paa represents the depth of the aa pool (recessive mixed pool) derived from the dominant parent; Mab indicates that the ab pool (dominant mixed pool) originates from the depth of the recessive parents; Pab represents the depth of ab pool (dominant mixed pool) derived from dominant parents.

Transcriptome Sequencing

The stems of *Actinidia chinensis* cv. HY-1 and *Actinidia eriantha* cv. MH-1 plants at 40 days of germination were sampled to extract RNA for RNA-seq. Total RNA from sampled leaves was extracted using RNA prep pure Plant Kit (Tiangen, Beijing, China), and then was reverse transcribed using Goldenstar RT6 cDNA Synthesis Kit Ver 2 (Tsingke, Beijing, China). The library construction and sequencing were carried out at Beijing Qingke Biotechnology Co., ltd. (Beijing, China) using Illumina HiSeq Platform (Illumina, USA). Gene expres sion levels were estimated by fragments per kilobase of transcript per million fragments mapped on Actinidia chinensis Hongyang v3 genome. The false discovery rate (FDR) < 0.01 and |log2(fold change)|≥ 1 was set as the threshold for genes showed significant differential expression. Gene Ontology (GO) enrichment analysis of differentially expressed genes (DEGs) was implemented by the GOseq R packages based on Wallenius non-central hyper-geometric distribution (Li et al. 2021). KEGG pathway enrichment analysis of the DEGs was completed by using KOBAS software to test the statistical enrichment of differential expression genes in KEGG pathways (Mao et al. 2005). The heatmaps of DEGs was drawn using TBtools software (v2.052) (Chen et al. 2023).

Subcellular localization

The fusion gene pHB-*AcbHLH1*-GFP, driven by the 35S promoter was constructed using the Golden Gate method, with Bsa I restriction enzyme. The recombinant construct, with the NLS-mCherry control vector, was transformed into Agrobacterium tumefaciens strain GV3101 respectively using the freeze-thaw method. The Agrobacterium suspensions containing the target and marker proteins were mixed at a 1:1 ratio and infiltrated into *Nicotiana benthamiana* leaves using a needleless syringe, followed by incubation under low-light conditions for 48 h. Green and red fluorescence signals were subsequently observed and recorded using confocal laser scanning microscopy (Zeiss LSM710/780).

Construction of overexpression vectors and plant transformation

The full-length coding sequence (CDS) of *AcbHLH1* was PCR-amplified from *Actinidia chinensis* cv. HY-1 leaf cDNA using T8 high-fidelity DNA polymerase (Beijing Tsingke Biotech Co., Ltd.), and the resulting product was double-digested

with HindIII and ScaI restriction enzymes before being ligated into the pHB binary vector. The recombinant plasmid was introduced into Agrobacterium tumefaciens strain GV3101 via freeze-thaw method, and subsequently used for to *Nicotiana benthamiana* leaf disctransformation under sterile conditions. Following transformation, the infected leaf discs were co-cultured on a co-culture medium, followed by screening and rooting cultures to generate trans genic plants. Genomic DNA was extracted from transgenic and wild-type (control) plants using CTAB, and subsequently used for PCR-based transgene identification. All primer sequences are listed in Table S7. T_1 generation seedlings were screened on MS medium supplemented with 10 mg L^{-1} kanamycin for herbicide resistance selection. After harvesting the seeds of T_1 generation plants, the seeds were dried at 28 ℃ for 24 hours and subjected to low-temperature dark treatment at 4 ℃ for 3 days before vernalization. The seeds were then sown and transplanted into a sterilized plastic pot ((10 cm diameter × 12 cm height) filled with media containing nutrient soil (Xianghuinon gke, China) and vermiculite (Baituji, China) at 2:1 (v:v). All plants were grown in artificial climate chamber at 0% relative humidity, with 25 ℃ (day for 12 h)/22 ℃ (night for 12 h) of light photoperiod with 100 μmol m^{-2} s^{-1}. The obtained plants were T_2 generation plants.

Observation of trichome lengh and density

Leaf samples at equivalent developmental stages and sizes were collected from both overexpression and wild-type plants, and subsequently stained with 2.5 % (w/v) glutaraldehyde solution for 120 min at room temperature. Wash tissue blocks with 0.1 M PB (pH 7.4) for 3 times, 15 min each. Then transfer tissue blocks into 1% OsO_4 in 0.1 M PB (pH 7.4) for 1-2 h at room temperature. After that, wash tissue blocks in 0.1 M PB (pH 7.4) for 3 times, 15 min each. The length and densities of the trichome were observed using a VHX-7000 microscope (hitachi, Japan). For quantitative analysis, three 1mm^2 regions (the upper, middle, and lower leaf sections) were selected per sample. Trichomes in each region were photographed and counted three times, with the final length and density expressed as the mean value of these measurements.

Supplementary Information

Table S1 Quality control of sequencing data for MH-1, HY-1 and bulked LD-pool and SD-pool samples.

Table S2 Information of the association regions.

Table S3 Annotation of SNPs in BSA-Seq.

Table S4 Statistics of SNP annotation.

Table S5 The whole genome sequencing reports of samples for RNA-seq.

Table S6 Annotation of SNPs in candidate interval.
Table S7 Sequences of primers used in the study.

Data availability
All data sheets and figures to process data are available upon request to the first author, Jiale Tang (tangjiale@hunaas.cn). Sequence data generated for this study is available publicly in the NCBI Sequence Read Archive under BioProject ID: PRJNA1493836.

Author Contributions
Jiale Tang, Ping Yuan designed the project. Jiale Tang managed the experiments with the help of Mengjie Chen, Ping Yuan, Kejia He, Fanwen Bu, Rencai Wang, Feixiong Luo, Hai Xu. Jiale Tang writing a draft of the manuscript. Jiale Tang revised the manuscript. Jiale Tang and Ping Yuan reviewed & edited the manuscript. All authors approved the article. All authors have read and agreed to the published version of the manuscript.

Funding
This work was financially supported by China Agriculture Research System of MOF and MARA (grant No. CARS-26) to Fanwen Bu, Modern Agriculture (Fruit) Industry Technology System of Hunan Province (grant No.HARS-09) to Hai Xu, and Agricultural Science & Technology Innovation Project of Hunan Province (grant No. 2025CX90) to Ping Yuan.

Acknowledgement

We thank all labmates in the kiwifruit breeding and cultivation team lab of Hunan Horticulture Research Institute for their generous help.

Declarations

Ethics approval and consent to participate
Not applicable.

Consent for publication
Not applicable.

Competing interest
The authors declare that they have no conflict of interest. The authors alone are responsible for the content and composition of this paper.

References

Ahmad Khan R, Mohammad, Kumar A, Abbas N (2024) AaGL3-like is jasmonate-induced bHLH transcription factor that positively regulates trichome density in Artemisia annua. Gene 904:148213. https://doi.org/10.1016/j.gene.2024.148213

Alahakoon UI, Taheri A, Nayidu NK, et al (2016) Hairy Canola (Brasssica napus) re-visited: Down-regulating TTG1 in an AtGL3-enhanced hairy leaf background improves growth, leaf trichome coverage, and metabolite gene expression diversity. BMC Plant Biol 16:12. https://doi.org/10.1186/s12870-015-0680-5

Amada G, Kobayashi K, Izuno A, et al (2020) Leaf trichomes in Metrosideros polymorpha can contribute to avoiding extra water stress by impeding gall formation. Annals of Botany 125:533–542. https://doi.org/10.1093/aob/mcz196

Bhandari DR, Wang Q, Friedt W, et al (2015) High resolution mass spectrometry imaging of plant tissues: towards a plant metabolite atlas. Analyst 140:7696–7709. https://doi.org/10.1039/C5AN01065A

Chen C, Wu Y, Li J, et al (2023) TBtools-II: A “one for all, all for one” bioinformatics platform for biological big-data mining. Molecular Plant 16:1733–1742. https://doi.org/10.1016/j.molp.2023.09.010

Chen Y, Su D, Li J, et al (2020) Overexpression of bHLH95, a basic helix–loop–helix transcription factor family member, impacts trichome formation via regulating gibberellin biosynthesis in tomato. Journal of Experimental Botany 71:3450–3462. https://doi.org/10.1093/jxb/eraa114

Fambrini M, Pugliesi C (2019) The Dynamic Genetic-Hormonal Regulatory Network Controlling the Trichome Development in Leaves. Plants 8:253. https://doi.org/10.3390/plants8080253

Fekih R, Takagi H, Tamiru M, et al (2013) MutMap+: Genetic Mapping and Mutant Identification without Crossing in Rice. PLoS ONE 8:e68529. https://doi.org/10.1371/journal.pone.0068529

Feng H, Guo L, Wang G, et al (2015) The Negative Correlation between Fiber Color and Quality Traits Revealed by QTL Analysis. PLoS ONE 10:e0129490. https://doi.org/10.1371/journal.pone.0129490

Fu Y, Li M, Huang L, et al (2026) Identification and knockout of SlHDZIV14 reveals fruit trichome-associated control of postharvest water loss in tomato. Postharvest Biology and Technology 237:114306. https://doi.org/10.1016/j.postharvbio.2026.114306

Gan L, Xia K, Chen J-G, Wang S (2011) Functional characterization of TRICHOMELESS2, a new single-repeat R3 MYB transcription factor in the regulation of trichome patterning in Arabidopsis. BMC Plant Biol 11:176. https://doi.org/10.1186/1471-2229-11-176

Harker FR, Jaeger SR, Lau K, Rossiter K (2007) CONSUMER PERCEPTIONS AND PREFERENCES FOR KIWIFRUIT: A REVIEW. Acta Hortic 81–88. https://doi.org/10.17660/ActaHortic.2007.753.7

Heng S, Li X, Li M, et al (2025) Two novel alleles of the MYB transcription factor *BjA06.GL1* and *BjB02.GL1* control leaf trichomes and enhance resistance to aphids in *Brassica juncea*. Horticulture Research 12:uhae314. https://doi.org/10.1093/hr/uhae314

Heydarian Z, Harrington M, Hegedus DD (2024) Defects in Glabrous 3 (GL3) functionality underlie the absence of trichomes in *Brassica napus*. The Plant Journal 119:1703–1719. https://doi.org/10.1111/tpj.16878

Kirik V, Lee MM, Wester K, et al (2005) Functional diversification of *MYB23* and *GL1* genes in trichome morphogenesis and initiation. Development 132:1477–1485. https://doi.org/10.1242/dev.01708

Kirik V, Simon M, Huelskamp M, Schiefelbein J (2004) The ENHANCER OF TRY AND CPC1 gene acts redundantly with TRIPTYCHON and CAPRICE in trichome and root hair cell patterning in Arabidopsis. Developmental Biology 268:506–513. https://doi.org/10.1016/j.ydbio.2003.12.037

Li F, Liu X, Ge H, et al (2021) Transcriptome profiling and differential expression analysis of the immune-related genes during the early phase of acute infection with Aeromonas hydrophila in the Chinese sucker (Myxocyprinus asiaticus). Aquaculture 545:737258. https://doi.org/10.1016/j.aquaculture.2021.737258

Li SF, Milliken ON, Pham H, et al (2009) The *Arabidopsis* MYB5 Transcription Factor Regulates Mucilage Synthesis, Seed Coat Development, and Trichome Morphogenesis. The Plant Cell 21:72–89. https://doi.org/10.1105/tpc.108.063503

Liang G, He H, Li Y, et al (2014) MYB82 functions in regulation of trichome development in Arabidopsis. Journal of Experimental Botany 65:3215–3223. https://doi.org/10.1093/jxb/eru179

Mao X, Cai T, Olyarchuk JG, Wei L (2005) Automated genome annotation and pathway identification using the KEGG Orthology (KO) as a controlled vocabulary. Bioinformatics 21:3787–3793. https://doi.org/10.1093/bioinformatics/bti430

McKenna A, Hanna M, Banks E, et al (2010) The Genome Analysis Toolkit: A MapReduce framework for analyzing next-generation DNA sequencing data. Genome Res 20:1297–1303. https://doi.org/10.1101/gr.107524.110

Méndez-Vigo B, Arteaga N, Murillo-Sánchez A, et al (2024) The bHLH transcription factor gene *EGL3* accounts for the natural diversity in Arabidopsis fruit trichome pattern and morphology. Plant Physiology 197:kiae673. https://doi.org/10.1093/plphys/kiae673

Meng Y, Lyu X, Liu J, et al (2023) Structural variation of GL1 gene determines the trichome

formation in Brassica juncea. Theor Appl Genet 136:75. https://doi.org/10.1007/s00122-023-04301-5

Miao T, Bao H, Ling H, et al (2023) Comparative Transcriptomic Analysis Revealed the Suppression and Alternative Splicing of Kiwifruit (Actinidia latifolia) NAP1 Gene Mediating Trichome Development. IJMS 24:4481. https://doi.org/10.3390/ijms24054481

Morohashi K, Grotewold E (2009) A Systems Approach Reveals Regulatory Circuitry for Arabidopsis Trichome Initiation by the GL3 and GL1 Selectors. PLoS Genet 5:e1000396. https://doi.org/10.1371/journal.pgen.1000396

Morohashi K, Zhao M, Yang M, et al (2007) Participation of the Arabidopsis bHLH Factor GL3 in Trichome Initiation Regulatory Events. Plant Physiology 145:736–746. https://doi.org/10.1104/pp.107.104521

Payne CT, Zhang F, Lloyd AM (2000) *GL3* Encodes a bHLH Protein That Regulates Trichome Development in Arabidopsis Through Interaction With GL1 and TTG1. Genetics 156:1349–1362. https://doi.org/10.1093/genetics/156.3.1349

Peng C, Yao X, Fu X, et al (2025) Evolution of short trichomes and long hairs on Nigella petals through co-option of bHLH and non-MIXTA MYB genes. Nat Commun 16:8304. https://doi.org/10.1038/s41467-025-64028-3

Qi X, Han F, Luo L, et al (2026) Structural Diversification of Actinidia Trichomes and Modulation by Polyploidization. Horticulturae 12:322. https://doi.org/10.3390/horticulturae12030322

Richardson DP, Ansell J, Drummond LN (2018) The nutritional and health attributes of kiwifruit: a review. Eur J Nutr 57:2659–2676. https://doi.org/10.1007/s00394-018-1627-z

Sm W, M A, Sa M, et al (2017) A Review of Production and Processing of Kiwifruit. J Food Process Technol 8:. https://doi.org/10.4172/2157-7110.1000699

Takagi H, Abe A, Yoshida K, et al (2013) QTL -seq: rapid mapping of quantitative trait loci in rice by whole genome resequencing of DNA from two bulked populations. The Plant Journal 74:174–183. https://doi.org/10.1111/tpj.12105

Wang S, Kwak S-H, Zeng Q, et al (2007) TRICHOMELESS1 regulates trichome patterning by suppressing *GLABRA1* in *Arabidopsis*. Development 134:3873–3882. https://doi.org/10.1242/dev.009597

Wester K, Digiuni S, Geier F, et al (2009) Functional diversity of R3 single-repeat genes in trichome development. Development 136:1487–1496. https://doi.org/10.1242/dev.021733

White J (1986a) Ontogeny and morphology of ovarian and fruit hairs in Kiwifruit. New Zealand

Journal of Botany 24:403–414. https://doi.org/10.1080/0028825X.1986.10409818

White J (1986b) Morphology of the fruit hairs in cultivars of *Actinidia deliciosa* var. *deliciosa Actindia eriantha* , and *Actinidia rufa*. New Zealand Journal of Botany 24:415–423. https://doi.org/10.1080/0028825X.1986.10409819

Wu M, Chang J, Han X, et al (2023) A HD-ZIP transcription factor specifies fates of multicellular trichomes via dosage-dependent mechanisms in tomato. Developmental Cell 58:278-288.e5. https://doi.org/10.1016/j.devcel.2023.01.009

Yang L, Wu Y, Jin J, et al (2025) An atypical bHLH transcription factor NtPRE4.1 negatively regulates tobacco glandular trichome density. Gene 962:149575. https://doi.org/10.1016/j.gene.2025.149575

Yu X, Qu M, Wu P, et al (2025) Super pan-genome reveals extensive genomic variations associated with phenotypic divergence in Actinidia. Mol Horticulture 5:4. https://doi.org/10.1186/s43897-024-00123-1

Yuan Y, Xu X, Luo Y, et al (2021) R2R3 MYB-dependent auxin signalling regulates trichome formation, and increased trichome density confers spider mite tolerance on tomato. Plant Biotechnology Journal 19:138–152. https://doi.org/10.1111/pbi.13448

Zhao H, Wang X, Zhu D, et al (2012) A Single Amino Acid Substitution in IIIf Subfamily of Basic Helix-Loop-Helix Transcription Factor AtMYC1 Leads to Trichome and Root Hair Patterning Defects by Abolishing Its Interaction with Partner Proteins in Arabidopsis. Journal of Biological Chemistry 287:14109–14121. https://doi.org/10.1074/jbc.M111.280735

Zheng J, Wu Y, Zhang L, et al (2025) Overexpression of NtMYB306c reduces the glandular trichomes density in tobacco. Biochemical and Biophysical Research Communications 772:152061. https://doi.org/10.1016/j.bbrc.2025.152061

Zheng S, Wang Y, Qu D, et al (2022) Study on population structure of kiwifruit and GWAS for hairiness character. Gene 821:146276. https://doi.org/10.1016/j.gene.2022.146276

Supplementary Files

This is a list of supplementary files associated with this preprint. Click to download.

- Additionalfiles.rar
- Additionalfiles.rar
- Additionalfiles.rar
- Additionalfiles.rar
- AcbHLH1.jpg
- AcbHLH1.jpg
- AcbHLH1.jpg
- AcbHLH1.jpg